# Interfacial self-assembly of a bacterial hydrophobin

Keith M. Bromley[a], Ryan J. Morris[a], Laura Hobley[b], Giovanni Brandani[a], Rachel M. C. Gillespie[b], Matthew McCluskey[a], Ulrich Zachariae[c], Davide Marenduzzo[a], Nicola R. Stanley-Wall[b,1], and Cait. E. MacPhee[a,1]

[a]School of Physics and Astronomy, University of Edinburgh, Edinburgh EH9 3FD, United Kingdom; [b]Division of Molecular Microbiology, College of Life Sciences, University of Dundee, Dundee DD1 5EH, United Kingdom; and [c]Division of Computational Biology, College of Life Sciences, University of Dundee, Dundee DD1 5EH, United Kingdom

Edited by Gregory A. Petsko, Weill Cornell Medical College, New York, NY, and approved March 24, 2015 (received for review October 2, 2014)

**The majority of bacteria in the natural environment live within the confines of a biofilm. The Gram-positive bacterium *Bacillus subtilis* forms biofilms that exhibit a characteristic wrinkled morphology and a highly hydrophobic surface. A critical component in generating these properties is the protein BslA, which forms a coat across the surface of the sessile community. We recently reported the structure of BslA, and noted the presence of a large surface-exposed hydrophobic patch. Such surface patches are also observed in the class of surface-active proteins known as hydrophobins, and are thought to mediate their interfacial activity. However, although functionally related to the hydrophobins, BslA shares no sequence nor structural similarity, and here we show that the mechanism of action is also distinct. Specifically, our results suggest that the amino acids making up the large, surface-exposed hydrophobic cap in the crystal structure are shielded in aqueous solution by adopting a random coil conformation, enabling the protein to be soluble and monomeric. At an interface, these cap residues refold, inserting the hydrophobic side chains into the air or oil phase and forming a three-stranded β-sheet. This form then self-assembles into a well-ordered 2D rectangular lattice that stabilizes the interface. By replacing a hydrophobic leucine in the center of the cap with a positively charged lysine, we changed the energetics of adsorption and disrupted the formation of the 2D lattice. This limited structural metamorphosis represents a previously unidentified environmentally responsive mechanism for interfacial stabilization by proteins.**

BslA | interfacial self-assembly | bacterial hydrophobin | *Bacillus subtilis* | biofilm

In the natural environment the majority of bacteria live within the confines of a structured social community called a biofilm. Residence offers bacteria multiple advantages over their free-living cousins that cannot be explained by genetics (1). Many of these benefits are conferred by production of an extracellular matrix, the hallmark feature of biofilms. The biofilm matrix largely consists of proteins, polysaccharides, and DNA. It provides a source of water and nutrients, and confers structural integrity (1–4). Biofilms formed by the Gram-positive bacterium *Bacillus subtilis* are characterized by a highly wrinkled morphology and a hydrophobic surface. The biofilm matrix is composed of a large exopolysaccharide synthesized by the products of the *epsA-O* operon, and the TasA/TapA proteins that form fibrous aggregates (5). Assembly of the matrix requires the small, secreted surface-active protein called BslA (formerly YuaB). BslA is found as a discrete layer at the surface of the biofilm despite uniform transcription of the coding region by the entire biofilm population (6–9). It achieves its surface hydrophobicity due to its striking amphiphilic structure, which we recently elucidated by X-ray crystallography (10). The structure of BslA consists of a canonical Ig-like domain, to which is appended a three-stranded "cap" that is highly hydrophobic in character, rich in leucine residues as well as isoleucine, valine, and alanine (10). In the crystal structure, this cap comprises a surface-exposed hydrophobic patch of ∼1,620 Å that we have previously proposed to mediate adsorption to the air/water interface.

The large surface-exposed hydrophobic patch exhibited by BslA is a characteristic shared by the unrelated family of fungal proteins known as the hydrophobins (11). Hydrophobins are a conserved family of surface-active proteins that, among other functions, lower the surface tension of growth medium, allowing fungal hyphae to penetrate the air–water interface. The hydrophobins are divided into class I and class II; class I proteins form robust amyloid-like rodlets at the air–water interface, whereas class II proteins reduce surface tension by forming ordered lattices of native-like protein at the interface. In both classes, eight canonical cysteine residues form a highly conserved series of disulfide bridges that provide a rigid framework that restricts the mobility of the polypeptide chain (12, 13). In the class II hydrophobins, this framework is thought to stabilize the surface exposure of the large hydrophobic patch that mediates interfacial assembly (14). The presence of a large hydrophobic patch on the surface of BslA, combined with its biological function, caused us to classify BslA as a bacterial hydrophobin; however, it shares neither sequence nor structural similarity. An outstanding question remains, therefore: in the absence of a stabilizing disulfide-bonded network, how is the large surface-exposed hydrophobic patch of BslA stabilized sufficiently in aqueous environments to mediate the surface activity of the protein?

Here we use WT-BslA and a targeted mutation in the cap domain (L77K) to determine the mechanism that enables BslA to partition from the aqueous phase to the interface, where it decreases the interfacial tension and self-assembles to form an ordered rectangular 2D protein lattice. We chose the L77K mutation for further investigation as it exhibits one of the most dramatic changes in interfacial activity both in vivo and in vitro (10), thus enabling us to determine the mechanism of action. We show that BslA undergoes an environmentally responsive conformational change: the cap is stabilized in aqueous solution by

## Significance

**In the natural environment the majority of bacteria live within the confines of a structured social community called a biofilm. The stability of biofilms arises from the extracellular matrix, which consists of proteins, polysaccharides, and extracellular DNA. One of these proteins, BslA, forms a hydrophobic "raincoat" at the surface of the biofilm. We have uncovered the mechanism that enables this protein to function, revealing a structural metamorphosis from a form that is stable in water to a structure that prefers the interface where it self-assembles with nanometer precision to form a robust film. Our findings have wide-ranging implications, from the disruption of harmful bacterial biofilms to the generation of nanoscale materials.**

Author contributions: K.M.B., R.J.M., L.H., G.B., U.Z., D.M., N.R.S.-W., and C.E.M. designed research; K.M.B., R.J.M., L.H., G.B., R.M.C.G., M.M., D.M., and C.E.M. performed research; L.H., G.B., and N.R.S.-W. contributed new reagents/analytic tools; K.M.B., R.J.M., L.H., G.B., R.M.C.G., M.M., U.Z., D.M., and N.R.S.-W. analyzed data; and K.M.B., R.J.M., L.H., N.R.S.-W., and C.E.M. wrote the paper.

The authors declare no conflict of interest.

This article is a PNAS Direct Submission.

Freely available online through the PNAS open access option.

[1]To whom correspondence may be addressed. Email: cait.macphee@ed.ac.uk or n.r.stanleywall@dundee.ac.uk.

This article contains supporting information online at www.pnas.org/lookup/suppl/doi:10.1073/pnas.1419016112/-/DCSupplemental.



BIOPHYSICS AND COMPUTATIONAL BIOLOGY

www.manaraa.com

burying the hydrophobic side chains in a random coil conformation, but switches to a surface-exposed hydrophobic β-sheet at an interface. This switch gives rise to a small energy barrier to adsorption, and both structural forms are represented in the decameric crystal structure. By mutating a single residue in the cap, we abolish the energy barrier, and although the cap region of the mutant protein still undergoes a coil-to-β-sheet transition at an interface, formation of the organized 2D lattice is disrupted. Taken together, our findings represent a previously undiscovered structural metamorphosis that enables interfacial stabilization by proteins.

## Results

Here we address the question of how the large surface-exposed hydrophobic patch of BslA is stabilized in aqueous environments to mediate the surface activity of the protein. One possible trivial mechanism is the formation of higher order oligomers, such as the decamer observed in the BslA crystal structure, or the tetramer observed for the class II fungal hydrophobin HFB II (15). However, although size exclusion chromatography indicated that purified BslA forms a mixture of monomers, dimers, and higher order oligomers (*SI Appendix*, Figs. S1 and S2), addition of a reducing agent such as dithiothreitol or β-mercaptoethanol yielded a sample containing purely monomeric protein (*SI Appendix*, Figs. S2 and S3) stable on the timescale of days. BslA contains two closely spaced cysteine residues, and the role of these residues in biofilm formation and/or maturation is as yet unclear. That said, here we show that the oxidation state of the cysteine residue is not important to the in vitro biophysical properties of the protein; dimeric BslA gives equivalent results to that of monomer if we assume that the concentration of surface-active species comprises 50% of the protein in the sample (i.e., only one subunit of the disulfide-bonded dimer is available for surface activity; *SI Appendix*, Fig. S4). We have therefore established that the monomeric protein is stable and soluble over a timescale of days, suggesting that the large hydrophobic cap we observed in the crystal structure must be shielded in aqueous solution, likely through some form of structural rearrangement. All experiments presented here used monomeric protein unless otherwise stated.

**WT-BslA Has a Barrier to Adsorption to an Air–Water Interface, Whereas BslA-L77K Does Not.** We know that the hydrophobic patch identified in the BslA crystal structure is important for interfacial activity, because mutations in this region affect both biofilm phenotype and partitioning to an oil–water interface (10). That BslA is stable as a monomer in aqueous solution suggests that the hydrophobic residues of the cap are not surface exposed, and there must be a conformational change to expose the hydrophobic patch, with a corresponding energy barrier to adsorption. To investigate this experimentally, pendant drop tensiometry with drop shape analysis was performed on BslA solutions at concentrations between 0.01 and 0.1 mg·mL$^{-1}$. In this technique, the shape of a drop is fitted to the Young–Laplace equation to measure the interfacial tension (IFT) at the droplet surface (16, 17), which decreases as the interface is populated by surface-active species (18). An increase in the error of the fit to the Young–Laplace equation indicates that a viscoelastic film has formed at the interface, and because a solid layer now separates the two liquid phases the concept of interfacial tension no longer applies (19). At low protein concentrations, the IFT initially remains unchanged for a lag time that is designated regime I (20, 21). During this period, the interface becomes occupied by protein to a critical surface coverage above 50% (20), and provides a measure of the rate at which the protein partitions to the interface. During regime II, the IFT decreases steeply until the interface is saturated with adsorbed protein, following which the IFT levels off (regime III), although a shallow gradient often indicates rearrangement of the protein layer. These characteristics can be seen in typical BslA dynamic interfacial tension response curves, however the fit error of the Young–Laplace equation to the droplet increased at some point during most experiments, indicating the formation of a viscoelastic layer (19).

The time ($t$) it takes for a particle to adsorb onto an interface via diffusion can be predicted by Eq. **1** (22):

$$\Gamma(t) = 2C_b\sqrt{\frac{Dt}{\pi}}, \qquad [1]$$

where Γ is surface concentration, $C_b$ is bulk concentration, and $D$ is the diffusion coefficient of the particle. Eq. **1** assumes that $C_b$ is unchanging and that there is no back diffusion from the interface (22). We can estimate $\Gamma_{max}$ (for 100% surface coverage) to be 1.57 mg·m$^{-2}$ from transmission electron microscopy (TEM) images of the BslA 2D lattice (*vide infra*; Fig. 3*A*), while $D$ was measured to be $9.87 \times 10^{-7}$ cm$^2$·s$^{-1}$ for monomeric BslA using dynamic light scattering (*SI Appendix*, Fig. S5). In cases where the error of the Laplace fit increased before a decrease in IFT was observed, then the onset time of any increase in the error of the Laplace fit was used (*SI Appendix*, Fig. S6).

Fig. 1 shows a plot of regime I time against BslA concentration for WT-BslA as well as the "ideal" regime I times calculated from Eq. **1** (Fig. 1, dashed line). The results clearly demonstrate that WT-BslA is slower to decrease the interfacial tension of a droplet (or increase the error of Laplace fit) in air than would be expected for a system that did not exhibit an adsorption barrier or back diffusion. If, however, we introduce a mutation into the cap region that replaces Leucine at position 77 with Lysine (L77K), the mutant showed no adsorption barrier, reducing the interfacial tension of the droplet within the maximum calculated time for particles of equivalent size (Fig. 1). Under diffusion-limiting conditions (Eq. **1**) BslA at a concentration of 0.03 mg·mL$^{-1}$ should take 22 s to reach a surface concentration of 1.57 mg·m$^{-2}$. As the IFT will begin to decrease at a surface coverage below 100%, BslA should require less than 22 s to reduce the IFT of a droplet. At 0.03 mg·mL$^{-1}$ the regime I time for WT-BslA was 97 ± 18 s, compared with 12 ± 4 s for BslA-L77K, confirming that BslA-L77K adsorption is purely diffusion limited, whereas WT-BslA faces an additional barrier to adsorption. This finding is consistent with the hypothesis that the WT protein undergoes a conformational change before adsorption. This energy barrier is not high, as dimensional analysis suggests that it is in the order of ~10 $k_BT$ (*SI Appendix*, Fig. S8), consistent with a limited structural rearrangement. We infer that introducing the positively charged lysine disrupts the conformation in aqueous solution so that not all of the hydrophobic groups pack optimally, and their partial exposure facilitates the interaction with the interface, abolishing the barrier to adsorption.

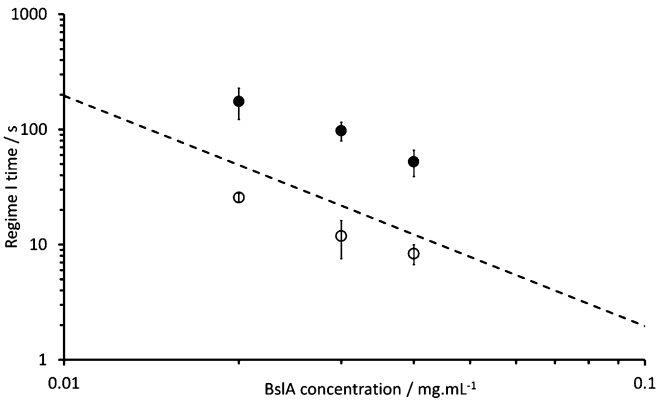


**Fig. 1.** A plot of regime I times versus concentration of WT-BslA (closed circles) and BslA-L77K (open circles). The dashed line represents the predicted time to reach a surface coverage of 1.57 mg·m$^{-2}$ using Eq. **1**.



www.manaraa.com

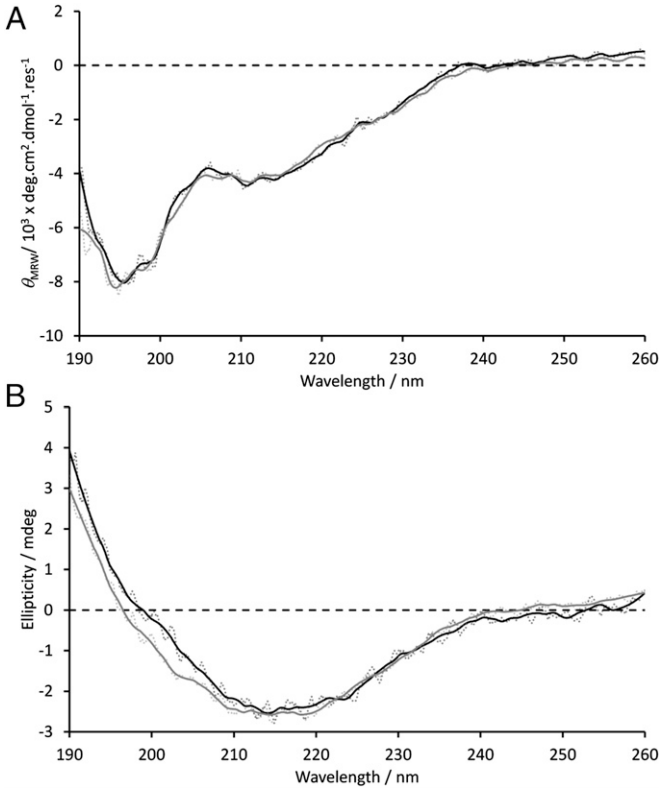


**Fig. 2.** (*A*) CD spectra of WT-BslA (black line) and BslA-L77K (gray line) in 25 mM phosphate buffer (pH 7). (*B*) CD spectra of refractive index matched emulsions stabilized by WT-BslA (black line) and BslA-L77K (gray line). Dotted lines: raw data; solid lines: smoothed data (*SI Appendix*).

**BslA Undergoes a Conformational Change to a Structure Enriched in β-Sheet upon Binding to an Oil–Water Interface.** What is the nature of the energy barrier against adsorption to the interface? To study the conformation of BslA in aqueous solution and at an oil–water interface, circular dichroism (CD) spectroscopy of WT-BslA was performed in aqueous solution and in refractive index matched emulsions (23). Refractive index matching enables the generation of oil-in-water emulsions without the light scattering that interferes with spectroscopic measurements. The CD spectrum of WT-BslA at pH 7 in phosphate buffer exhibited a maximum at ∼205 nm, a minimum at ∼212 nm, and a shoulder at ∼226 nm (Fig. 2*A*). The minimum at ∼212 nm is consistent with some β-sheet structure, whereas the minimum at <200 nm suggests a significant contribution from random coil. On binding to the interface of decane–water emulsions, the CD spectrum of WT-BslA is substantially altered (Fig. 2*B*), exhibiting a positive signal below 200 nm and a minimum at 215–218 nm. Such features indicate a structural change to a form enriched in β-sheet (24). Qualitative modeling of CD spectra derived from "ideal" secondary structural elements is consistent with only a small proportion (∼10%) of the protein undergoing a structural change (*SI Appendix*, Fig. S9).

We have shown that BslA-L77K shows no energy barrier to adsorption (Fig. 1), which suggests that some of the hydrophobic groups buried in the cap region of WT-BslA are more surface exposed, and that any structural transition has a lower energy barrier associated with it. This is consistent with the lysine residue at position 77 adopting an orientation that solvates it (pointing out rather than in), perhaps distorting other amino acids that make up the cap and making them available to interact with the interface. Surprisingly, CD spectroscopy of BslA-L77K shows very similar behavior to the wild-type protein, with a substantial contribution from random coil in aqueous solution converting to β-sheet at the interface. Unfortunately, CD spectroscopy is unable to distinguish between different forms of random coil in aqueous solution; however, the observation of β-sheet structure at an interface is unexpected.

**WT-BslA Forms a Highly Ordered 2D Rectangular Lattice at the Air–Water Interface, Whereas the BslA-L77K Molecules Are More Disordered.** Having established that BslA undergoes a structural transition, we next examined the structure of the film formed at an interface by TEM. WT-BslA forms a highly ordered rectangular lattice (Fig. 3*A*). Multiple domains of the WT-BslA lattice could be observed in any location on the grid. The observed domain areas varied from as small as 1,000 nm$^2$ (∼50 BslA molecules) up to 200,000 nm$^2$ (>10,000 BslA molecules). Less ordered "interdomain" areas were also observed. Performing a fast Fourier transform (FFT) on TEM images of WT-BslA (Fig. 3*A*, *Inset*) revealed a rectangular lattice ($\alpha = \beta = 90°$, $a \neq b$) with dimensions of $d$ (10) = 3.9 nm and $d$(01) = 4.3 nm. Thus, when the cap is in the β-sheet form, the protein self-assembles in 2D; we suggest that this may be mediated via formation of an extended intermolecular hydrogen-bonded β-sheet.

In contrast to the wild-type protein, TEM images of BslA-L77K revealed a predominantly disorganized arrangement of protein, which nonetheless contained rectangular packed patches (Fig. 3*B*). The largest BslA-L77K domain size observed was ∼20,000 nm$^2$ (∼1,250 BslA molecules). FFT on ordered domains of BslA-L77K revealed lattice parameters [$d$ (10) = 3.9 nm, $d$(01) = 4.3 nm, $\alpha = \beta = 90°$] identical to the WT-BslA lattice (Fig. 3*B*, *Inset*). Thus, although the CD data suggests that the L77K mutant undergoes a random-coil to β-sheet transition similar to that of the wild-type protein, the ability of the folded protein to self-assemble laterally into ordered domains is impaired. That some domains are observed suggests that the impaired packing can be overcome; nonetheless the microscopy analysis argues that the β-sheet formed by the cap region of the L77K mutant is either less stable or more dynamic—consistent with the insertion of a positively charged amino acid into a hydrophobic environment. This is also consistent with our previous data demonstrating that L77K is easily displaced from a biological or in vitro interface, whereas the wild-type protein is not (10).

**The Crystal Structure of Decameric BslA Reveals Two Distinct Structural Forms.** From the data presented thus far, we suggest that the cap region of monomeric BslA is a random coil in aqueous solution with the hydrophobic side chains buried; at an interface the cap restructures to form a β-sheet, and self-assembles into a 2D lattice. Further supporting data for this model comes from the X-ray crystal structure (10): analysis reveals two substantially different cap configurations in the decameric repeat unit (Fig. 4*A*). Eight of the ten subunits are positioned with their caps in close proximity in a micelle-like arrangement. In these proteins, the cap regions are in a β-sheet configuration with the hydrophobic residues oriented

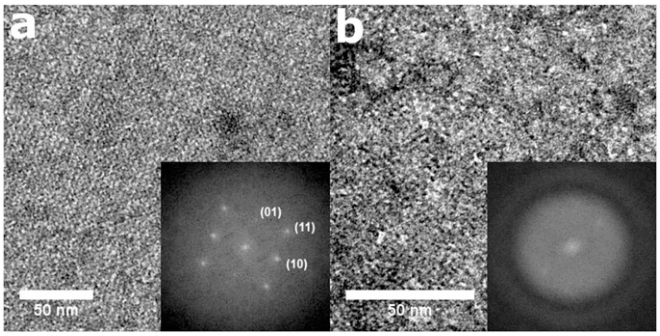


**Fig. 3.** TEM images of (*A*) WT-BslA and (*B*) BslA-L77K stained with uranyl acetate. Scale bar = 50 nm. *Insets*: FFTs of the entire TEM image. The numbers in *A* correspond to the Miller indices of the 2D lattice structure.





www.manaraa.com

outward (Fig. 4*B*), creating the oily core of the micelle. The remaining two subunits (chains I and J) are farther away from the center of the decamer and the cap regions are in a random coil configuration with many of the hydrophobic side chains oriented away from the solvent (Fig. 4*B*). Taken together, our findings are consistent with chains A–H representing the interfacially bound form, and chains I and J the structure adopted in aqueous solution. This difference highlights the structural plasticity of the cap region, which undergoes substantial rearrangement in different solvent environments.

The crystal structure of BslA indicates that the majority of the protein adopts a β-sheet structure; however, the region encompassing amino acids 94–111 forms a partially structured loop. We cannot rule out the possibility that this region also restructures at an interface, contributing to the increase in β-sheet content observed by CD, however systematic mutagenesis reveals that mutations in this region have no in vivo phenotypic consequences (T94A; K95M; D96N; T97A; L98A; N99A; A102M; L103A; R104M; L109A; N110S; N111S) (*SI Appendix*, Fig. S7). Thus, if this region restructures, it has no functional consequence with respect to hydrophobicity or self-assembly of BslA, processes that underpin successful biofilm assembly.

**Mechanism of Insertion and Self-Assembly of BslA at an Interface.** Next, to make quantitative estimates of the energetic consequences of having two structural forms of BslA, we used coarse-grained molecular dynamics simulations. Initially, for WT-BslA, the free energy of adsorption was reconstructed from pulling simulations by making use of the Jarzynski equality (25, 26) (see *SI Appendix* for full description of methods). Our calculations show that the β-sheet cap configuration (chain C in the crystal structure) favorably increased the free energy of binding of BslA to the interface compared with the random coil cap configuration (chain I), despite the fact that the two forms are chemically identical. Specifically, the calculated free energy of adsorption ($\Delta G$) of chain C was 107.9 ± 0.7 $k_BT$; whereas, the $\Delta G$ of chain I was just over half this value, at 59.3 ± 0.7 $k_BT$. Thus, the more structured form of the protein with a surface-exposed hydrophobic patch is more tightly adsorbed to the interface, even in the absence of intermolecular interactions. The large difference in $\Delta G$ between WT-BslA chain C and chain I supports the hypothesis that chain C represents the conformation at the interface, and chain I represents the structure of BslA in solution. Moreover, the average orientation of the longest axis of the two forms of the protein at the interface was significantly different: chain C positioned itself at an angle of ∼29.5° to the normal; whereas, chain I was significantly tilted at ∼55.0°. We hypothesize that the less tilted conformation facilitates interprotein interactions in the interfacial lattice.

Substituting the leucine at position 77 for lysine reduced $\Delta G$ for chain C to 85.2 ± 0.6 $k_BT$, although $\Delta G$ for L77K chain I (59.5 ± 0.6 $k_BT$) was similar to WT-BslA. Chains C and I of BslA-L77K were oriented at similar angles to the corresponding WT chains. If we make the simplifying assumption that chain C represents the interfacial form of the protein and chain I the form in aqueous solution, and ignore energetic contributions arising from structural rearrangements (which in any case appear to be small), the $\Delta\Delta G$ associated with interfacial partitioning is 48.6 $k_BT$ for the wild-type protein and 25.7 $k_BT$ for the mutant, which provides additional insight into the comparative ease with which the L77K mutant is removed from the interface following film compression. However, to make a comparison between the two proteins in our simulations, we directly replaced Leu-77 with lysine with no concomitant structural changes. Given that the introduction of the lysine eliminates the barrier to adsorption at the interface it is likely that the mutation causes some rearrangement of the cap and an increased exposure of neighboring hydrophobic amino acids. Thus, the $\Delta G$ for the chain I form of L77K is likely to be an underestimate, and the $\Delta\Delta G$ for L77K an overestimate.


**Fig. 4.** (*A*) The secondary structures of chain C and chain I of BslA, derived from the crystal structure PDB: 4BHU (10). Color code: β-strand (blue), α-helix (magenta), residue Leu-77 (green), cap strands (yellow highlight). Amino acids 43–46, 155–159, and 171–172 of chain I are not defined in the crystal structure, suggesting structural heterogeneity. (*B*) A depiction of chain C (*Left*) and chain I (*Right*), highlighting the different orientations of the hydrophobic residues in the cap (black). Images generated using Visual Molecular Dynamics (33).

**Functional Consequences of BslA Activity.** BslA functions in vivo to aid in the erection of aerial structures in the biofilm (10, 27), a role that is suggestive of the capability to reduce the surface tension of water. Pendant drop tensiometry was performed on aqueous droplets of BslA to observe the change in interfacial tension over time.

Fig. 5*A* shows the change in IFT of droplets of unfractionated WT-BslA suspended in air and in oil. The magnitude of the decrease in IFT caused by BslA was consistently smaller than the typical drop in IFT observed for the class II fungal hydrophobin HFBII at similar concentrations and timescales (19). This is perhaps not surprising as even a small energy barrier associated with a structural rearrangement has a significant impact on adsorption kinetics. For example, at 0.02 mg·mL$^{-1}$ and 300 s, BslA decreases the apparent IFT to 70.8 ± 1 mN·m$^{-1}$; whereas, HFBII decreases the IFT to ∼56 mN·m$^{-1}$ under the same conditions (19). However, despite this comparatively small decrease in IFT, an increase in the error of the Laplace fit (*SI Appendix*, Fig. S6) indicates that a BslA film has already formed by 300 s, whereas HFBII must lower the IFT to at least 50 mN·m$^{-1}$ before the error of the Laplace fit increases (19).

Previously, the viscoelastic film formed by the class II fungal hydrophobin HFBI was shown to cause a sessile drop to develop a planar surface after 30 min on a hydrophobic material (28), indicating that the protein film formed at the interface has a sufficiently high elastic modulus as to deform the droplet shape (29). In contrast, WT-BslA does not deform sessile drops at 0.01, 0.03, and 0.1 mg·mL$^{-1}$ after 30 min, even though visual inspection confirmed the formation of a film in each case (Fig. 5*B*). The formation of such a film was confirmed at water–air or water–oil interfaces by the appearance of persistent wrinkles on the surface of pendant drops following compression (10).

Fig. 5 shows a WT-BslA droplet suspended in air (Fig. 5*C*) or oil (Fig. 5*D*) before and after compression. Taken together, our results indicate that the different mechanism of action of BslA has functional consequences: BslA forms interfacial films at lower protein densities than the class II fungal hydrophobins,



www.manaraa.com

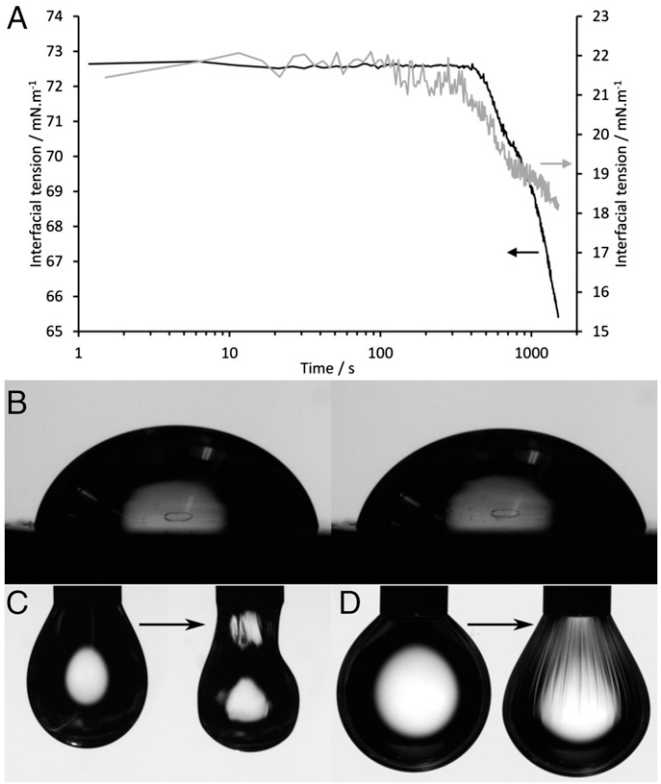


**Fig. 5.** (*A*) Interfacial tension profiles of a droplet of unfractionated WT-BslA (0.02 mg·mL$^{-1}$) in air (black line) and in glyceryl trioctanoate (gray line). (*B*) A 50-μL droplet of WT-BslA (0.03 mg·mL$^{-1}$) on highly ordered pyrolytic graphite after 0 (*Left*) and 30 (*Right*) min. (*C*) A 25-μL droplet of WT-BslA (0.02 mg·mL$^{-1}$) in air before and after compression. (*D*) A 40-μL droplet of WT-BslA (0.2 mg·mL$^{-1}$) in glyceryl trioctanoate before and after compression.

and the resulting films, although very stable, have an elastic modulus that does not deform the droplet shape. Such elasticity may enable BslA to uniformly coat the highly wrinkled morphology of the native *B. subtilis* biofilm.

At the interface BslA undergoes an environmentally responsive structural metamorphosis. Thus, the mechanism of stabilization of the hydrophobic patch in BslA is fundamentally different to that observed for the fungal hydrophobins: instead of the network of conserved disulfide bonds required to stabilize the energetically unfavorable surface exposure of hydrophobic amino acids observed in the hydrophobins, BslA has evolved structural plasticity in the three-stranded cap that allows conformational rearrangement. Only once the protein adsorbs to the interface do the residues within the cap refold to reach a free energy minimum in which the hydrophobic residues protrude into the nonaqueous phase. This structure–function relationship may be important for the function of BslA in vivo. As the BslA coding region is expressed throughout the entire *B. subtilis* biofilm population (8), the molecule needs to diffuse through the extracellular matrix to the surface of the biofilm without hindrance. A cap that becomes significantly more hydrophobic after adsorption would be a useful mechanism to help prevent unwanted interactions leading to retention of BslA within the body of the biofilm community. It should however be noted that this does not preclude other potential transport mechanisms to the biofilm interface such as the involvement of a chaperone protein. Moreover, these findings open up the possibility that the alternative conformational form of BslA has additional functions within the confines of the biofilm unrelated to its function in conferring hydrophobicity at the biofilm surface.

## Discussion

Details of the components that make up the biofilm matrix have been elucidated for several species of bacteria (1, 4). However, information at the molecular and biophysical level regarding how these molecules contribute to biofilm stability, and how they assemble in the three dimensions of the bacterial community is largely lacking. Here we have illuminated the mechanism by which BslA, a protein made by all members of the *B. subtilis* biofilm community, selectively assembles at the interface of the biofilm. This mechanism is summarized in Fig. 6 where a schematic for the adsorption of WT-BslA compared with BslA-L77K is depicted. In both cases, the monomeric protein adsorbs to the interface, although our data show that the rate of adsorption of BslA-L77K is greater as it experiences no barrier. After adsorption, both WT-BslA and BslA-L77K refold into structures enriched in β-sheet, but only WT-BslA can organize into an extensive, highly ordered 2D rectangular lattice. It is the high free energy of adsorption, combined with formation of a stable lattice structure that enhances the stability of WT-BslA interfacial films, so that introducing a small amount of compression is insufficient to remove WT-BslA from the interface (10). This is in contrast to BslA-L77K, which has a lower free energy of adsorption and does not form an organized lattice over the entire droplet surface, and is thus easily removed upon compression of the interface.

We performed all experiments on monomeric BslA, and moreover complementary experiments with dimeric BslA indicated that it is the monomeric unit that mediates the observed interfacial activity (*SI Appendix*, Fig. S4). Native BslA contains two cysteine residues toward the C terminus in a "C×C" motif, and we cannot rule out an additional stabilizing contribution

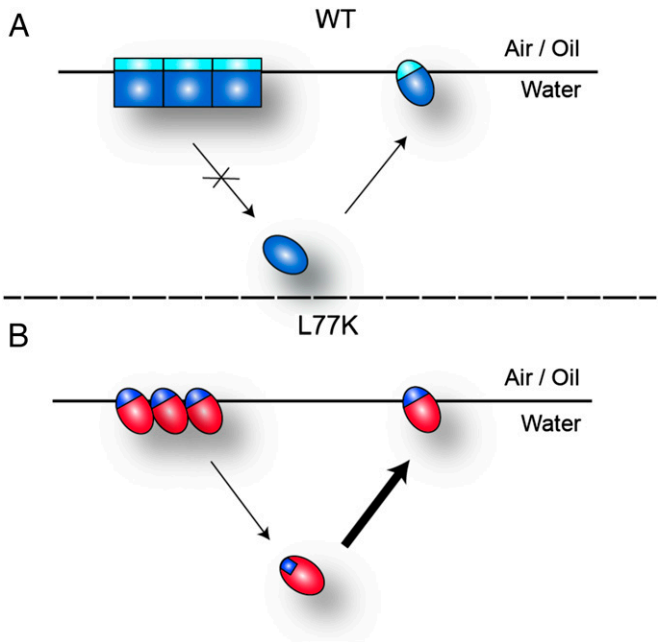


**Fig. 6.** Schematic of BslA adsorption. When unbound, the conformation of the hydrophobic cap of WT-BslA (*A*) orients the hydrophobic residues away from the aqueous medium, slowing the rate of adsorption (indicated by a small arrow). The L77K mutation (*B*) removes the adsorption barrier by exposing some or all of the hydrophobic residues within the hydrophobic cap, increasing the rate of adsorption (indicated by a bold arrow). Once adsorbed onto the interface, the surface-bound WT-BslA refolds to a conformation rich in β-sheet and is able to form strong lateral interactions with adjacent molecules, forming an organized lattice that under normal circumstances will not be removed from the interface (indicated by the crossed arrow). Surface-bound BslA-L77K forms a less well-organized lattice and can be removed from the interface with only minimal energy, such as droplet compression.





www.manaraa.com

from disulfide formation at the elevated local protein concentrations present in the interfacial layer. This is unlikely to be the origin of the observed difference in stability of WT-BslA and L77K-BslA films under compression, however, because the cysteines are unchanged. Moreover, our simulations show that the wild-type and mutant proteins are inserted into the interface in similar orientations and with the same tilt angle, suggesting that there is unlikely to be any orientational barrier to disulfide bond formation by the mutant protein at the interface. Nonetheless, the C×C motif may have functional consequences in the biofilm, either mediating interactions between BslA molecules, or interactions with other protein or polysaccharide components in the matrix. For example, the surface layer of BslA observed in the biofilm is clearly more than a single protein layer thick (10); BslA may function as a dimeric protein with one cap region interacting with the interface and the second mediating protein–protein interactions within the biofilm. One important consequence of the mechanism we have uncovered, however, is that if the protein is indeed dimeric, it is likely to be bifunctional: one of the caps may be β-sheet and hydrophobic and the second is random coil and stable in an aqueous or hydrophilic environment.

The amphiphilic nature of the fungal hydrophobins has led to suggestions for many potential applications, and these may be equally relevant to BslA. Hydrophobins have been proposed for use as surface modifiers and coating agents (30), and as emulsifiers, foam stabilizers, and surfactants in many application areas including the food industry (31). The slow kinetics of adsorption will be an important factor to consider when attempting to use BslA in any applications, particularly where other surfactants are present. It has been shown, for example, that class I hydrophobins adhere more strongly to interfaces than the class II proteins, but that the class II species can successfully compete to form a mixed interfacial membrane (32). Unlike BslA, however, class II hydrophobins exhibit no barrier to interfacial adsorption, whereas the rapid adsorption of any competing species is likely to modulate BslA interfacial activity. Nonetheless, the structured self-assembly of BslA offers many opportunities for surface modification with nanoscale control.

## Materials and Methods

Full details of all methods used are provided in *SI Appendix*.

**Protein Purification.** BslA was purified after expression as a GST fusion protein using standard techniques. See *SI Appendix* for full details.

**Circular Dichroism Spectropolarimetry.** CD was performed using a Jasco J-810 spectropolarimeter. Control samples were analyzed at a concentration of 0.1 $mg{\cdot}mL^{-1}$ (6.7 μM) in a 0.1-cm quartz cuvette. Refractive index matched emulsions were analyzed in a 0.01-cm demountable quartz cuvette. Measurements were performed with a scan rate of 50 $nm{\cdot}s^{-1}$, a data pitch of 0.1 nm, and a digital integration time of 1 s.

**Pendant Drop Tensiometry.** Monitoring the kinetics of BslA adsorption was achieved using pendant drop tensiometry with drop shape analysis. A Krüss Easydrop tensiometer (Krüss GmbH) was used in combination with Drop Shape Analysis software. See *SI Appendix* for full details.

**Transmission Electron Microscopy.** BslA-WT and L77K samples were deposited onto carbon-coated copper grids (Cu-grid) (TAAB Laboratories Equipment, Ltd.) and imaged using a Philips/FEI CM120 BioTwin transmission electron microscope. See *SI Appendix* for full details.

**ACKNOWLEDGMENTS.** We thank the Edinburgh Protein Production (Biophysical Characterisation) Facility for use of circular dichroism spectroscopy and Dr. Colin Hammond for assistance with the size exclusion chromatography–multiangle laser light scattering experiment. This work was supported by Engineering and Physical Sciences Research Council Grant EP/J007404/1 and Biotechnology and Biological Sciences Research Council Grants BB/L006979/1, BB/I019464/1, and BB/L006804/1. Mass-spectrometry analysis of purified proteins was performed in the College of Life Sciences and is supported by the Wellcome Trust 097945/B/11/Z.

1. Flemming H-C, Wingender J (2010) The biofilm matrix. *Nat Rev Microbiol* 8(9): 623–633.
2. Costerton JW, Lewandowski Z, Caldwell DE, Korber DR, Lappin-Scott HM (1995) Microbial biofilms. *Annu Rev Microbiol* 49:711–745.
3. Davey ME, O'Toole GA (2000) Microbial biofilms: From ecology to molecular genetics. *Microbiol Mol Biol Rev* 64(4):847–867.
4. Cairns LS, Hobley L, Stanley-Wall NR (2014) Biofilm formation by Bacillus subtilis: New insights into regulatory strategies and assembly mechanisms. *Mol Microbiol* 93(4): 587–598.
5. Vlamakis H, Chai Y, Beauregard P, Losick R, Kolter R (2013) Sticking together: Building a biofilm the Bacillus subtilis way. *Nat Rev Microbiol* 11(3):157–168.
6. Branda SS, Chu F, Kearns DB, Losick R, Kolter R (2006) A major protein component of the Bacillus subtilis biofilm matrix. *Mol Microbiol* 59(4):1229–1238.
7. Kearns DB, Chu F, Branda SS, Kolter R, Losick R (2005) A master regulator for biofilm formation by Bacillus subtilis. *Mol Microbiol* 55(3):739–749.
8. Ostrowski A, Mehert A, Prescott A, Kiley TB, Stanley-Wall NR (2011) YuaB functions synergistically with the exopolysaccharide and TasA amyloid fibers to allow biofilm formation by Bacillus subtilis. *J Bacteriol* 193(18):4821–4831.
9. Kobayashi K, Iwano M (2012) BslA(YuaB) forms a hydrophobic layer on the surface of Bacillus subtilis biofilms. *Mol Microbiol* 85(1):51–66.
10. Hobley L, et al. (2013) BslA is a self-assembling bacterial hydrophobin that coats the Bacillus subtilis biofilm. *Proc Natl Acad Sci USA* 110(33):13600–13605.
11. Linder MB, Szilvay GR, Nakari-Setälä T, Penttilä ME (2005) Hydrophobins: The protein-amphiphiles of filamentous fungi. *FEMS Microbiol Rev* 29(5):877–896.
12. Wösten H, De Vries O, Wessels J (1993) Interfacial self-assembly of a fungal hydrophobin into a hydrophobic rodlet layer. *Plant Cell* 5(11):1567–1574.
13. De Vries OMH, Fekkes MP, Wösten HAB, Wessels JGH (1993) Insoluble hydrophobin complexes in the walls of Schizophyllum commune and other filamentous fungi. *Arch Microbiol* 159:330–335.
14. Hakanpää J, et al. (2006) Two crystal structures of Trichoderma reesei hydrophobin HFBI—The structure of a protein amphiphile with and without detergent interaction. *Protein Sci* 15(9):2129–2140.
15. Torkkeli M, Serimaa R, Ikkala O, Linder M (2002) Aggregation and self-assembly of hydrophobins from Trichoderma reesei: Low-resolution structural models. *Biophys J* 83(4):2240–2247.
16. Andreas JM, Hauser EA, Tucker WB (1938) Boundary tension by pendant drops. *J Phys Chem* 42(8):1001–1019.
17. Stauffer CE (1965) The measurement of surface tension by the pendant drop technique. *J Phys Chem* 69(6):1933–1938.
18. Rosen MJ (2004) *Surfactants and Interfacial Phenomena* (Wiley, Hoboken, NJ), 3rd Ed.
19. Alexandrov NA, et al. (2012) Interfacial layers from the protein HFBII hydrophobin: Dynamic surface tension, dilatational elasticity and relaxation times. *J Colloid Interface Sci* 376(1):296–306.
20. Tripp BC, Magda JJ, Andrade JD (1995) Adsorption of globular protein at air/water interface as measured by dynamic surface tension: Concentration dependence, mass-transfer considerations, and adsorption kinetics. *J Colloid Interface Sci* 173:16–27.
21. Beverung CJ, Radke CJ, Blanch HW (1999) Protein adsorption at the oil/water interface: Characterization of adsorption kinetics by dynamic interfacial tension measurements. *Biophys Chem* 81(1):59–80.
22. Ward AFH, Tordai L (1946) Time-dependence of boundary tensions of solutions I. The role of diffusion in time-effects. *J Chem Phys* 14(7):453–461.
23. Husband FA, Garrood MJ, Mackie AR, Burnett GR, Wilde PJ (2001) Adsorbed protein secondary and tertiary structures by circular dichroism and infrared spectroscopy with refractive index matched emulsions. *J Agric Food Chem* 49(2):859–866.
24. Towell JF, III, Manning MC (1994) Analysis of protein structure by circular dichroism spectroscopy. *Analytical Applications of Circular Dichroism*, eds Purdie N, Brittain HG (Elsevier, New York), pp 175–205.
25. Jarzynski C (1997) Nonequilibrium equality for free energy differences. *Phys Rev Lett* 78(14):2690–2693.
26. Park S, Schulten K (2004) Calculating potentials of mean force from steered molecular dynamics simulations. *J Chem Phys* 120(13):5946–5961.
27. Kobayashi K (2007) Gradual activation of the response regulator DegU controls serial expression of genes for flagellum formation and biofilm formation in Bacillus subtilis. *Mol Microbiol* 66(2):395–409.
28. Szilvay GR, et al. (2007) Self-assembled hydrophobin protein films at the air-water interface: Structural analysis and molecular engineering. *Biochemistry* 46(9):2345–2354.
29. Jang H-S, et al. (2014) Tyrosine-mediated two-dimensional peptide assembly and its role as a bio-inspired catalytic scaffold. *Nat Commun* 5:3665.
30. Valo HK, et al. (2010) Multifunctional hydrophobin: Toward functional coatings for drug nanoparticles. *ACS Nano* 4(3):1750–1758.
31. Hektor HJ, Scholtmeijer K (2005) Hydrophobins: Proteins with potential. *Curr Opin Biotechnol* 16(4):434–439.
32. Askolin S, et al. (2006) Interaction and comparison of a class I hydrophobin from Schizophyllum commune and class II hydrophobins from Trichoderma reesei. *Biomacromolecules* 7(4):1295–1301.
33. Humphrey W, Dalke A, Schulten K (1996) VMD: Visual molecular dynamics. *J Mol Graph* 14(1):33–38, 27–28.



www.manaraa.com